PHYSICAL REVIEW B VOLUME 24, NUMBER 9 1 NOVEMBER 1981

Hamiltonian studies of the $d=2$ Ashkin-Teller model

Mahito Kohmoto,* Marcel den Nijs, and Leo P. Kadanoff
The James Franck Institute, The University of Chicago, Chicago, Illinois 60637
(Received 2 March 1981)

We study a one-dimensional quantum Hamiltonian problem which is equivalent to a highly anisotropic version of the two-dimensional Ashkin-Teller model. This problem is studied by using its duality and other symmetry properties, by a consideration of its limiting cases, and by mapping it into an XXZ linear chain which is equivalent to a highly anisotropic six-vertex model. In addition eleventh-order strong-coupling series are used to derive numerical data about the Hamiltonian problem. By these means a phase diagram is obtained. The essentially new feature of this diagram is a "critical fan," i.e., a region where a line of continuously varying criticality "fans out" and becomes an area of critical behavior.

I. INTRODUCTION

The two-dimensional Ashkin-Teller model[1] is one of the models which have a line of continuously varying critical indices. This model has four states per site and may be useful to describe magnetic systems with two easy axes. It is also a prototype which is useful for understanding other two dimensional problems. To define this model, we use a statistical variable $\theta(\vec{r})$, defined on the lattice points, which takes four different values

$$\theta(\vec{r})=0,\quad \pi/2,\quad \pi,\quad 3\pi/2\ . \tag{1.1}$$

The partition function is

$$Z=\mathrm{Tr}_{\theta(\vec{r})}\exp(-H)\ . \tag{1.2}$$

In the anisotropic case, we define the action, H, to take the form

$$\begin{aligned}H=-\sum_{\vec{r}}\{&2K_2^x\cos[\theta(\vec{r})-\theta(\vec{r}+\hat{x})]\\&+K_4^x\cos[2\theta(\vec{r})-2\theta(\vec{r}+\hat{x})]\\&+2K_2^\tau\cos[\theta(\vec{r})-\theta(\vec{r}+\hat{\tau})]\\&+K_4^\tau\cos[2\theta(\vec{r})-2\theta(\vec{r}+\hat{\tau})]\}\ .\end{aligned} \tag{1.3}$$

Here $\vec{r}=(j,k)$ is the set of all lattice sites on a square lattice, while $\hat{x}=(1,0)$ and $\hat{\tau}=(0,1)$ are nearest-neighbor displacement vectors on this lattice. We employ the notation τ for the y direction in preparation for a consideration of the highly anisotropic (τ) limit of Kogut.[2]

The K_2's and K_4's in Eq. (1.3) are called two- and four-spin coupling constants. This language refers to an alternative Ising-variable description of the Ashkin-Teller model in which two variables $S(\vec{r})=\pm1$ and $T(\vec{r})=\pm1$ are placed at each lattice site. The combination of these two variables makes four possible states at each site, which corresponds to the four values of $\theta(\vec{r})$ in Eq. (1.1). The correspondence is listed in Table I. The action can be expressed in terms of these Ising variables since

$$\begin{aligned}&2\cos[\theta(\vec{r})-\theta(\vec{r}')]=S(\vec{r})S(\vec{r}')+T(\vec{r})T(\vec{r}')\ ,\\&\cos[2\theta(\vec{r})-2\theta(\vec{r}')]=S(\vec{r})S(\vec{r}')T(\vec{r})T(\vec{r}')\ .\end{aligned} \tag{1.4}$$

Thus, the Ashkin-Teller model can be thought as two Ising models coupled by a four-spin interaction. At $K_4=0$ the model reduces to two decoupled Ising models with nearest-neighbor couplings K_2. From the Onsager solution[3] we know that a second-order phase transition takes place and the specific heat diverges logarithmically; i.e., the critical exponent α is equal to zero.

Another point at which an additional symmetry occurs is when the two- and four-spin couplings are equal, $K_2^x=K_4^x$ and $K_2^\tau=K_4^\tau$. Then each bond takes the form $4K_2(\delta_{\theta,\theta'}-\frac{1}{4})$, and the problem becomes the four-state Potts model. This model also has a

TABLE I. The correspondence between the variable θ and the Ising variables S and T.

θ	S	T	ST	$\cos\theta=\frac{S+T}{2}$	$\cos2\theta=ST$
0	1	1	1	1	1
$\pi/2$	1	−1	−1	0	−1
π	−1	−1	1	−1	1
$3\pi/2$	−1	1	−1	0	−1

second-order phase transition,[4] but with critical indices which differ from the Ising values.[5–7] In the isotropic case,[5,6,8] and indeed more generally,[9,10] it is known that these two special-symmetry second-order transitions are connected by a line of continuously varying critical behavior.

In this paper, an extremely anisotropic version of the Ashkin-Teller model is studied using the time-continuum Hamiltonian formalism.[2] An advantage of the quantum Hamiltonian is the simpler geometry of the one-dimensional system which may be expected to lead to a problem which is at once more understandable and also more easily analyzed via, for example, series techniques. The two-dimensional classical model is reduced to a one-dimensional quantum model by taking the extreme lattice anisotropic limit $(K_2^x,K_4^x)\to 0$, $(K_2^\tau,K_4^\tau)\to\infty$. This limit is rather subtle and can be performed in many ways. We choose the particular parameterization of the couplings

$$K_2^x=\tau\beta\ ,\quad K_4^x=\tau\beta\lambda\ ,$$
$$K_2^\tau=\tfrac{1}{4}(\ln\tau^{-1}-\ln\lambda)\ ,\quad K_4^\tau=\tfrac{1}{4}(\ln\tau^{-1}+\ln\lambda)\ . \tag{1.5}$$

and take $\tau\to 0$ to enforce the anisotropy. As shown in Sec. II below, the transfer-matrix method may be used to convert the statistical mechanics problem defined by Eq. (1.3) into a ground-state problem for the quantum Hamiltonian.

In the limit defined by Eqs. (1.5), $\mathcal{H}$ reads

$$\mathcal{H}=\sum_j[2(1-\cos p_j)+\lambda(1-\cos 2p_j)] -\beta\sum_j[2\cos(\theta_j-\theta_{j+1})+\lambda\cos 2(\theta_j-\theta_{j+1})]\ . \tag{1.6}$$

The operator θ_j acts on a site j and has four eigenvalues: 0, $\pi/2$, π, and $\frac{3}{2}\pi$. Its conjugate operator p_j changes the eigenstates of the operator θ_j as

$$e^{inp_j}|\theta_j\rangle=|\theta_j+n\pi/2\rangle\ . \tag{1.7}$$

Here n is any integer and θ_j is defined modulus additions or subtractions of integer multiples of 2π.

As we shall see in Sec. II, $\mathcal{H}$ has particularly nice symmetry properties which we have obtained by enforcing the special form of the anisotropic limit. In the Appendix, we derive mappings between our model [Eq. (1.6)] and the staggered six vertex model and the staggered XXZ Heisenberg chain problem, respectively. Our choice of anisotropy limit is necessary so that the special case $\beta=1$ gives a model which is equivalent to the (exactly solved) unstaggered version of these problems.[11] This result is then used in Sec. III as a starting point to pin down the phase diagram of our quantum version of the Ashkin-Teller model. As we show in this section, its entire structure can be constructed with the help of our knowledge of the six vertex model and of other exactly soluble limiting cases. In Sec. IV, strong-coupling series expansions are used to verify and further specify this phase diagram.

For the reader who might be particularly interested in results rather than methodology, we show here the phase diagram of the ground state of the Hamiltonian (1.6) as derived in Sec. III together with some of the supporting series data of Sec. IV (see Fig. 1). This phase diagram shows five main regions:

(a) A paramagnetic region, labeled I, in which there is no ordering and hence zero average values of $e^{i\theta}$ and $e^{2i\theta}$.

(b) A fully ordered region, III, in which one of the four possible values of θ appears preferentially in the ground state so that $e^{i\theta}$ gains an expectation value.

(c) A partially ordered region, II in which pairs of θ values [i.e., (0 and π) or ($-\pi/2$ and $\pi/2$)] appear preferentially in the ground state. Here $e^{2i\theta}$ will gain an expectation value, but the average of $e^{i\theta}$ will remain zero.

(d) An antiferromagnetic frozen region, region IV, in which the system may be divided into two sublattices and the sublattices behave differently. On one sublattice, $e^{2i\theta}$ and e^{2ip} have, respectively, eigenvalues 1 and -1. On the other both have eigenvalues -1. In this region also, the average of $e^{i\theta}$ vanishes.

(e) Finally the shaded area is an extended region of criticality which we call a critical fan. The averages of $e^{i\theta}$ and $e^{2i\theta}$ vanish. However, throughout the entire region correlation functions decay algebraically in space and other typical features of critical behavior are seen. In this domain, critical indices vary from point to point in a continuous fashion.

This diagram can be further appreciated by con-

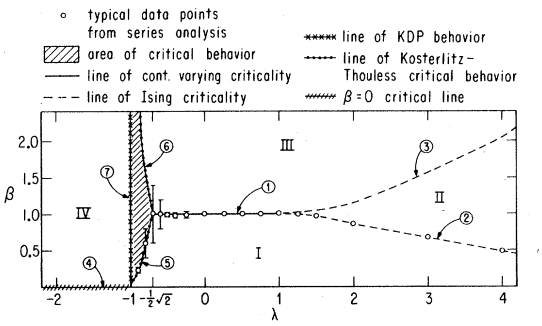

FIG. 1. Phase diagram of the anisotropic limit of the $d=2$ Ashkin-Teller model from studies of the $d=1$ quantum Hamiltonian. Estimates of critical points by a series analysis are shown with error bars. For those without an error bar, the apparent error is smaller than the size of the plotted point.

trasting it with the phase diagram of the isotropic Ashkin-Teller model ($K_2^x = K_2^\tau$, $K_4^x = K_4^\tau$) shown in Fig. 2. The qualitative features of regions I, II, and III are identical in the two pictures as is the topology of the diagrams in the right-hand half of the pictures. In the left-hand half of the picture for the isotropic case, region IV is once again a region of antiferromagnetic ordering of $e^{2I\theta}$. However, no critical fan appears in the isotropic case, and the topology on the left-hand sides of the pictures are entirely different.

We believe that the antiferromagnetic to paramagnetic transition (line 4 of Fig. 2) of the isotropic case has merged into the $\beta=0$ critical line of Fig. 1. A discussion of how this might occur as well as the structure of the phase diagram for negative values of β is reserved for a future publication.

The regions are separated by critical lines. Line number 1 in Fig. 1 and indeed the entire line $\beta=1$, is analyzed below by making use of an exact mapping of our model of Eq. (1.6) into the (exactly solved) six-vertex model. Continuously varying critical behavior is then shown to occur for all λ obeying $|\lambda|<1$. Critical indices are exactly evaluated as a function of λ. These conclusions are checked numerically in Sec. IV.

Lines 2 and 3 in both the isotropic and anisotropic cases are expected to be in the Ising model universality class. The critical fan is not seen in the isotropic phase diagram. If one walks along critical line 1 in Fig. 2 towards $K_4/K_2 \to -1$, one finds that the parameter λ takes the value $\lambda=-\frac{1}{2}$. The critical fan is located beyond the "horizon" where the Boltzmann weights have become negative. Also the boundaries of the critical fan, of course, do not appear in the isotropic case. Lines 5 and 6 are expected to be in the same universality class as the Kosterlitz-Thouless transition; line 7 is in the same class as the potassium dihydrogen phosphate (KDP) model.[11]

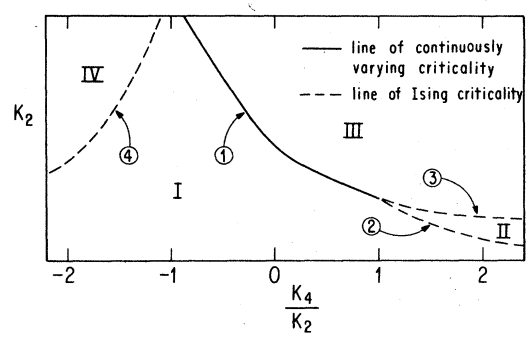

FIG. 2. Phase diagram of the isotropic $d=2$ Ashkin-Teller model.

II. TIME CONTINUUM LIMIT AND THE QUANTUM HAMILTONIAN

In this section, the quantum Hamiltonian for the Ashkin-Teller model is obtained.

Consider a N by M square lattice on which the θ variables are placed. The partition function (1.2) is written conveniently in terms of the transfer matrix

$$Z = \mathrm{Tr}\, V^N \ . \tag{2.1}$$

Here Tr is now a diagonal sum over a set of θ_j's ($j=1,2,\ldots,M$) in which the matrix V is given by

$$\langle \{\theta_i\}|V|\{\theta_i'\}\rangle = \exp\left(\sum_{j=1}^{M}[2K_2^x\cos(\theta_j-\theta_{j+1})+K_4^x\cos(2\theta_j-2\theta_{j+1})]\right) \times \exp\left(\sum_{j=1}^{M}\{2K_2^\tau[\cos(\theta_j-\theta_j')-1]+K_4^\tau[\cos(2\theta_j-2\theta_j')-1]\}\right) \ . \tag{2.2}$$

Here θ_j ($j=1,2,\ldots,M$) are the θ variables within one row and θ_j' are those in the adjacent row. Each θ_j takes four values,

$$\theta_j = 0,\ \pi/2,\ \pi,\ \tfrac{3}{2}\pi \ . \tag{2.3}$$

The matrix V connects the two rows. If we regard the transfer to the next row as the time evolution, the transfer matrix is closely related to the Hamiltonian $\mathcal{H}$. The relation is

$$V = \exp(-\tau\mathcal{H}) = 1-\tau\mathcal{H}+O(\tau^2) \ , \tag{2.4}$$

where τ is the lattice spacing in the time direction. In general this Hamiltonian $\mathcal{H}$ is a very complicated operator. However, in the limit (1.5) where the τ couplings go to infinity and the x couplings go to zero, it has a simple form. The diagonal element of V is obtained by setting $\theta_j=\theta_j'$ for $j=1,2,\ldots,$ and M and in the parametrization of Eq. (1.5) it can be written as

$$V_{\text{diag}}=\exp\left[\sum_{j=1}^{M}[2K_2^x\cos(\theta_j-\theta_{j+1})+K_4^x\cos(2\theta_j-2\theta_{j+1})]\right]=1+\tau\beta\sum_{j=1}^{M}[2\cos(\theta_j-\theta_{j+1})+\lambda\cos(2\theta_j-2\theta_{j+1})]+O(\tau^2)\ . \tag{2.5}$$

The off-diagonal matrix element where $\Delta\theta_k=\theta_k-\theta_k'=\pm\pi/2$ and $\Delta\theta_j=0(j\neq k)$ is written as

$$V_{\text{off}}(\Delta\theta_k=\pm\pi/2)=\exp(-2K_2^\tau-2K_4^\tau)=\tau\ . \tag{2.6}$$

Also the matrix element for $\Delta\theta_k=\pi$ and $\Delta\theta_j=0(j\neq k)$ is

$$V_{\text{off}}(\Delta\theta_k=\pi)=\exp(-4K_2^\tau)=\tau\lambda\ . \tag{2.7}$$

Other matrix elements which represent multiple excitations are higher than second order in τ. From Eqs. (2.5), (2.6), and (2.7), we can write V in an operator form

$$V=1+\tau\beta\sum_{j=1}^{M}[2\cos(\theta_j-\theta_{j+1})+\lambda\cos(2\theta_j-2\theta_{j+1})]+\tau\sum_{j=1}^{M}[2\cos p_j+\lambda\cos 2p_j]+O(\tau^2)\ , \tag{2.8}$$

where the operator p_j is conjugate to θ_j and has been defined in Eq. (1.7). Compare Eq. (2.8) with Eq. (2.4) in the $\tau\to 0$ limit. Apart from trivial additive constants, this gives

$$\mathcal{H}=-\beta\sum_j[2\cos(\theta_j-\theta_{j+1})+\lambda\cos(2\theta_j-2\theta_{j+1})]+\sum_j[2(1-\cos p_j)+\lambda(1-\cos 2p_j)]\ . \tag{2.9}$$

What we have to be careful about in this formalism is that the anisotropic limit must be taken so that the two systems represent the same physics. The parameterization of Eq. (1.5) ensures that the Hamiltonian (2.9) has a dual property. This duality is stated as

$$\tilde{p}_j=\theta_j-\theta_{j+1}\ , \tag{2.10}$$

$$\tilde{\theta}_j=\sum_{k>j}p_k\ , \tag{2.11}$$

$$\beta\mathcal{H}(1/\beta,\lambda;\tilde{\theta},\tilde{p})=\mathcal{H}(\beta,\lambda;\theta,p)\ . \tag{2.12}$$

The duality tells us that the structure of the phase diagram at $\beta>1$ is the same as that of $\beta<1$. Along the self-dual line $\beta=1$, this model can be mapped on the exactly soluble six-vertex model and, as shown in the Appendix the parametrization (1.5) is a necessary condition for this mapping. Another property of the Hamiltonian is

$$\mathcal{H}(\beta,\lambda;\theta,p)=-\mathcal{H}(\beta,-\lambda;\tilde{\theta}',\tilde{p}')\ . \tag{2.13}$$

From Eq. (2.9) follows that this statement is correct when we have a symmetry transformation R that changes only the sign of the $\cos(\theta_j-\theta_{j+1})$ term. The sign of the $\cos p_j$ term can then also be changed by the transformation $D^{-1}RD$; with D the duality transformation (2.10)–(2.12). The operator R which does this is the one that rotates the eigenstates of the θ_j operator at all odd sites over π: $\tilde{\theta}_j'=\theta_j+\pi$. Its action on the operator p_j at the odd sites is a reflection $p_j\to -p_j$. Since the Hamiltonian contains $\cos p_j$ and $\cos 2p_j$ terms this last effect of R does not change the Hamiltonian.

The relation (2.13) connects the regions $\lambda>0$ and $\lambda<0$. However the important difference from the duality relation (2.12) is the overall sign changes in Eq. (2.13). The ground state is mapped onto an excited state, and is different in those two regions. Therefore the phase structures are considerably different.

In addition to the properties (2.12) and (2.13) which relate different regions in the phase diagram, the Hamiltonian has invariant properties under the transformations of θ_j's. The symmetry group for these transformations is the dihedral group of order 4. At the special values of λ, the Hamiltonian acquires additional symmetries. At $\lambda=0$ the symmetry group can be thought of as $Z(2)\times Z(2)$. Therefore at this point the Hamiltonian represents two decoupled Ising models which have $Z(2)$ symmetries.

At $\lambda=1$, the symmetry group is the permutation group of order 4, and we have the four-state Potts model. The line $\lambda=-1$ is connected by Eq. (2.13) to the line $\lambda=1$ and we have also the permutation symmetry there. The line $\lambda=-1$ could be identified as the "antiferromagnetic" four-state Potts model.

However this line is beyond the horizon where ratios of Blotzmann weights become negative (see Sec. I) and we cannot see this line in the traditional parametrization of the four-state Potts model. As we will see all finite temperature behavior of the antiferromagnetic Potts model has, just as the Ising line 4 in Fig. 2, collapsed onto the point $\beta=0$ by the lattice anisotropy limit. This part of the phase diagram is given an extra singular behavior by the anisotropy limit.

III. PHASE DIAGRAM

In this section we discuss the evidence for the phase diagram of Fig. 1, that can be obtained from exact soluble limit cases and renormalization flow arguments.

A. Two critical lines of Ising type: Region $\lambda > 1$

The isotropic Ashkin-Teller critical line with continuously varying criticality bifurcates into two lines of the Ising type at the four-state Potts point.[7,8] In the present case of the anisotropic limit, the Hamiltonian (1.6) also shows this bifurcation. Line 1 in Fig. 1 splits at the four-state Potts point $\lambda=1$ into the two Ising-type critical lines 2 and 3. Line 2 can be understood by examining the limit $\lambda >> 1$, $\beta\lambda = O(1)$. In this limit the Hamiltonian (1.6) becomes

$$\mathcal{H} = \sum_j [\,\lambda(1-\cos 2p_j) + 2(1-\cos p_j) - \beta\lambda\cos(2\theta_j - 2\theta_{j+1})\,] \quad . \tag{3.1}$$

Since $\lambda >> 1$, the first term dominates and the system is restricted to take only the two states $p_i = 0$ and π at each site. The second and third terms then represent a quantum system with two levels at each site and with a nearest-neighbor interaction to flip the two levels. This is precisely the time-continuum Hamiltonian for the two-dimensional Ising model, which has a critical point at $\beta\lambda = 2$. The critical line 2 approaches asymptotically the line $\beta = 2/\lambda$ as λ becomes large. Below this line the system is in a disordered phase (region I in Fig. 1). Above this line, the system is partially ordered (region II). The Hamiltonian is dominated by the terms which are proportional to λ and becomes

$$\mathcal{H} = \lambda \sum_j [(1-\cos 2p_j) - \beta\cos(2\theta_j - 2\theta_{j+1})] \quad . \tag{3.2}$$

The ground state of this Hamiltonian is doubly degenerate and can be obtained exactly, because the operators $\cos 2p_i$ and $\cos(2\theta_j - 2\theta_{j+1})$ commute. The two ground-state eigenvectors are

$$\psi_+ = \prod_j (|0\rangle_j + |\pi\rangle_j) \quad , \tag{3.3}$$

and

$$\psi_- = \prod_j (|\pi/2\rangle_j + |\tfrac{3}{2}\pi\rangle_j) \quad , \tag{3.4}$$

where $|0\rangle_j$, $|\pi/2\rangle_j$, $|\pi\rangle_j$, and $|3\pi/2\rangle_j$ are the four eigenstates of the operator θ_j at the site j. The symmetry is partially spontaneously broken, since the system takes either the state ψ_+ or the state ψ_-. The expectation value of the polarization operator $\exp(2i\theta_j)$ is $+1$ or -1, respectively, in these two states (see Table I). The system, however, has not yet chosen between $|0\rangle$ and $|\pi\rangle$ or between $|\pi/2\rangle$ and $|-\pi/2\rangle$ at each site. So the expectation value of the magnetization $e^{\pm i\theta}$ still vanish.

In region III, the terms which are proportional to β dominate in the Hamiltonian. Accordingly all the spins tend to be in the same eigenstate $|0\rangle$, $|\pi/2\rangle$, $|\pi\rangle$, or $|3\pi/2\rangle$ of the operator θ_j. So, in region III the magnetization $e^{\pm i\theta}$ as well as the polarization $e^{2i\theta}$ are nonzero. The critical line 3 between the phases II and III is an Ising disorder-order transition with respect to the order parameters $e^{\pm i\theta}$. This line maps on line 2 by the duality transformation (2.10)–(2.12).

B. Antiferromagnetically frozen phase: Region $\lambda < -1$

For $\lambda << -1$, the Hamiltonian can again be represented by Eq. (3.2). The difference from the previous case $\lambda > 1$ is the overall sign. The ground state is neither ψ_+ nor ψ_-, but instead all spins at even sites are in the state $|0\rangle - |\pi\rangle$ and all spins at odd sites in $|\pi/2\rangle - |-\pi/2\rangle$ (or vice versa)

$$\psi_{\text{ant}} = \prod_j (|0\rangle_{2j} - |\pi\rangle_{2j})\,(|\pi/2\rangle_{2j+1} - |3\pi/2\rangle_{2j+1}) \quad . \tag{3.5}$$

In this ground state the polarization $e^{2i\theta}$ is antiferromagnetically ordered. In the isotropic model, this corresponds to the antiferromagnetic phase IV in Fig. 2. The whole finite temperature region in this part of Fig. 2 has in Fig. 1 collapsed into $\beta=0$, $\lambda < -1$. The anisotropy limit that we had to use in order to preserve the duality for line 1 is not suitable for this region. We find that for all $\beta > 0$, $\lambda < -1$ the model is "frozen," i.e., perfectly ordered.

The state ψ_{ant} is an eigenstate of the complete Ashkin-Teller Hamiltonian for all λ and β values. The terms which are neglected in the $|\lambda| \to \infty$ Hamiltonian (3.2) are $\cos p_j$ and $\beta\cos(\theta_j - \theta_{j+1})$. Both operators give zero when applied to the state ψ_{ant}. So

indeed we have an exact eigenstate of the Hamiltonian. The energy per spin is given by

$$E=\lambda(2+\beta)+2 \ . \tag{3.6}$$

For $\lambda << -1$ we already checked that this also happens to be the ground state. As long as the energy of one of the other eigenstates does not cross with this state, the model is perfectly ordered. This crossing happens at the line $\beta=0$ for $\lambda<-1$. At $\beta=0$ the Hamiltonian decouples and is trivially soluble. The energy eigenvalues at each decoupled site are

$$E=\begin{cases}0, & \text{for } p=0\\ 2\lambda+2, & \text{for } p=\dfrac{\pi}{2} \text{ and } \dfrac{3}{2}\pi\\ 4, & \text{for } p=\pi \ .\end{cases} \tag{3.7}$$

For $\lambda>-1$ every spin will choose the state $p_i=0$. So there the ground state is unique. For $\lambda<-1$, however the lowest energy is $2\lambda+2$. Here the ground state is 2^M times degenerate, and includes our state ψ_{ant}. In a trivial way the mass gap is zero, and the model can be considered to be critical. This is not completely unexpected, since the Ising line 4 in Fig. 2 has collapsed onto this section of the $\beta=0$ line because of the lattice anisotropy limit.

At $\lambda=-1$ the ground-state degeneracy becomes 3^M. We will argue below that this is the limit point of the critical fan (see Fig. 1). The other phase boundary of the frozen phase is the line $\lambda=-1$. As we will see below the transition here is KDP-like. This is a peculiar first-order phase transition which also shows a divergence in the specific heat from the $\lambda>-1$ side.[11]

C. Line of continuously varying critical indices and the critical fan

At $\beta=1$ the Hamiltonian reduces to the exactly soluble XXZ model. This is the quantum Hamiltonian for the six-vertex model.[12] For the isotropic case it is known that the Ashkin-Teller model can be mapped via a duality transformation onto a staggered six-vertex model.[6,13] This remains true also for the anisotropic model. At the self-dual line $\beta=1$ the staggering disappears, and the model reduces to the corresponding six-vertex model (see the Appendix, Sec. 1). In the Appendix Sec. 2 we give a direct way of rewriting the Ashkin-Teller Hamiltonian as a staggered XXZ model. For the details of the soluttion of the six-vertex model we refer to the review paper by Lieb and Wu.[11] The implications for the Ashkin-Teller Hamiltonian at $\beta=1$ are as follows. For all $|\lambda|<1$ the model is critical (i.e., massless in the quantum field language). The six-vertex model shows two types of transitions. At $\lambda=1$, i.e., the four-state Potts limit, we see the F-model type of transition. It is of infinite order. Nowadays we call this a Kosterlitz-Thouless transition. The singular part of the free energy (equal to the ground-state energy) behaves as

$$f\sim\exp(-b|\lambda-1|^{-1/2}) \ . \tag{3.8}$$

For $\lambda>1$ six-vertex model is in an antiferroelectrical ordered phase. In the Ashkin-Teller language this is seen as the partially ordered ferromagnetic state, with nonzero polarization (see Sec. III A).

For $\lambda<-1$ the six-vertex model is frozen in a perfectly ordered state that in that language is ferroelectrical. This agrees with our results of Sec. III B. The transition at $\lambda=-1$ is that of the KDP model. Since the ground state for $\lambda<<-1$ is also an eigenstate for all λ and β values (see Sec. III B), the transition must be obtained from a crossing of eigenstates. In general the first derivative of the ground-state energy at the crossing will show a jump. So it is not surprising that the transition at $\lambda=-1$ is found to be first order.[11] But that is not all. At the $\lambda>-1$ side the model is critical. The ground-state energy there behaves as $E_0\sim|\lambda+1|^{3/2}$. So superimposed on the first-order transition, the "specific heat" also diverges with the exponent $\alpha=\frac{1}{2}$ from this side.

Along the critical line $\beta=1$, $|\lambda|<1$ the critical indices vary continuously. In order to determine the precise dependency of the other exponents of the Ashkin-Teller model, we need the Baxter solution.[14] A temperature change in the eight-vertex model corresponds in the Ashkin-Teller language to a difference in the strength between the nearest-neighbor coupling K_2 for the S and T spins.[6] Therefore the critical index of this crossover operator in the Ashkin-Teller model is known from the Baxter's solution as

$$x_{\text{cr}}=x_T^{8V}=2-2\mu/\pi \ , \tag{3.9}$$

$$\cos\mu=\lambda \ . \tag{3.10}$$

Other critical indices are known from the extended scaling relations. The relations that are of interest in this paper are[15,16]

$$x_T x_{\text{cr}}=1 \ , \tag{3.11}$$

$$x_p=\tfrac{1}{4}x_T \ , \tag{3.12}$$

$$X_H=\tfrac{1}{8} \ . \tag{3.13}$$

Here x_T is the correlation function critical index of the energy operator $\cos(\theta_i-\theta_{i+1})$, x_p that of the electrical field (polarization) operator $e^{2i\theta}$, and x_H that of the magnetic field operator $e^{i\theta}$.

These relations have been obtained from mappings between the six-vertex model and the Gaussian model.[17–19] The equivalent mapping in the one-

dimensional quantum field language is that between the XXZ model and the Tomonaga-Luttinger model.[20–22] These critical indices relate to the free-energy exponents y_T, y_p, and y_{8V} as $2=x_i+y_i$.

Let us now concentrate on the value of the energy exponent y_T. When it becomes negative the structure of the phase diagram must change drastically. From Eqs. (3.9), (3.10), and (3.11) it follows that this is the case for $-1<\lambda<-\frac{1}{2}\sqrt{2}$.

When the exponent is relevant ($y_T>0$), the free energy behaves singularly as $|1-\beta|^{2/y_T}$. When the exponent is irrelevant, however ($y_T<0$), the model remains critical around $\beta=1$. Stated in the renormalization-group language: when $y_T>0$, the flow is away from $\beta=1$, when $y_T<0$ one flows inwards. All critical points that flow towards the same fixed point belong to the same universality class. So for $-1<\lambda<-\frac{1}{2}\sqrt{2}$ the critical line with continuously varying exponents at $\beta=1$ fans out into a critical fan.

We can write down renormalization-group equations that are valid locally around $\beta=1$. In the scaling limit the Ashkin-Teller Hamiltonian can be replaced by the Hamiltonian of the Gaussian model with spin-wave interactions[17–22]

$$H=\int d\vec{r}\,[K(\vec{\nabla}\phi)^2+(1-\beta)\cos 2\phi+u_4\cos 4\phi]\ . \tag{3.14}$$

Here one can think of u_4 as a fixed small constant. The coupling constant K is a known function of λ

$$K=\frac{2}{\pi}(1-\arccos\lambda/\pi)\ . \tag{3.15}$$

The $\cos 4\phi$ is the operator that drives the Kosterlitz-Thouless transition at $\lambda=1$ in the six-vertex model. It is generated in the scaling limit procedure, that leads to Eq. (3.14) by an umklapp process.[21,22] The $\cos 2\phi$ operator is the energy operator of the Ashkin-Teller model. For $\lambda<-\frac{1}{2}\sqrt{2}$ both $\cos 2\phi$ and $\cos 4\phi$ are irrelevant. There the Ashkin-Teller model looks Gaussian, i.e., is critical everywhere (the critical fan). At $\lambda=-\frac{1}{2}\sqrt{2}$, the $\cos 2\phi$ operator becomes relevant. So until $\lambda=1$, where the $\cos 4\phi$ becomes relevant too, the model only remains Gaussian at $\beta=1$. At $\lambda=-1$ the Gaussian analysis breaks down too. However it is not because of a Kosterlitz-Thouless mechanism. It is just the point where $K=0$ in Eq. (3.14).

Around the critical fan we are allowed to neglect the $\cos 4\phi$ interaction. Locally the renormalization-group equations are then those of Kosterlitz[23,24] (who originally derived them for the planar model)

$$\begin{aligned}\frac{d\lambda}{dl}&=-A(\beta-1)^2\ ,\\ \frac{d}{dl}(\beta-1)&=y_T(\beta-1)\ .\end{aligned} \tag{3.16}$$

We learn from this that the lines 5 and 6 in Fig. 1 are Kosterlitz-Thouless transition lines, and that these lines approach $\beta=1$ under a finite angle (that depends on A). Moreover the critical indices in the critical fan vary continuously and still satisfy the same extended scaling relations as at $\beta=1$.

The renormalization-group equations (3.16) are valid only for small $(\beta-1)$. They only determine the streamlines, along which the critical exponents do not change, up to first order in $(\beta-1)$. We need independent information to determine the shape of the critical fan for large values of $\beta-1$.

There is no indication of an abrupt ending of the fan. We expect it to contract itself into the point $\lambda=-1$ in the limit $\beta\downarrow 0$, because this is the only point at the $\beta=0$ axis where the ground state is 3^M-fold degenerate [see Eq. (3.7)].

The ultimate streamline that flows into the KDP point at $\beta=1$, $\lambda=-1$, is expected to be a straight line (at $\lambda=-1$), because of the extra permutation symmetry at $\lambda=-1$ (see Sec. II). Everywhere along this line the transition into the frozen phase (region IV in Fig. 1) will be KDP-like.

IV. HIGH-TEMPERATURE EXPANSIONS

A perturbation expansion of the Hamiltonian (1.6) for small values of β gives useful information about the critical properties of the system. This expansion corresponds to what is known in statistical mechanics as the high-temperature expansion. In particle physics, it is usually called strong-coupling expansion.

We need rather long series to investigate the critical region because usually the values of β are not small there. To deal with the high-order perturbations we apply the linked cluster expansion method proposed by Kadanoff and Kohmoto.[25] In this method, connected parts of wave functions are defined such that disconnected contributions are simply products of the connected parts. As a result, only the connected wave functions need to be evaluated. This method is particularly useful when we calculate disorder operators. These are string operators which in many cases are dual to usual order operators. In finite-size lattice calculations, we would need a lattice for the string operators twice as long as would be required for ground-state calculations. The lattice is effectively infinite in the linked cluster expansion because only the connected parts of the wave functions are calculated.

A. Description of the calculations

Here we briefly discuss the perturbation methods for free energies, magnetizations, and susceptibilities. For details of the methods, see Ref. 25.

1. Ground-state energy

The Hamiltonian (1.6) is written as

$$\mathcal{H} = T + \beta U \ , \tag{4.1}$$

where

$$T = \sum_j [2(1-\cos p_j) + \lambda(1-\cos 2p_j)] \ , \tag{4.2}$$

and

$$U = -\sum_j [2\cos(\theta_j - \theta_{j+1}) + \lambda \cos(2\theta_j - 2\theta_{j+1})] \ . \tag{4.3}$$

We call the unperturbed Hamiltonian T a kinetic energy and the perturbation U a potential. The kinetic energy is decoupled, and unperturbed wave functions take one of four eigenstates of the operator p_j, $|p=0\rangle$, $|p=\pi/2\rangle$, $|p=\pi\rangle$, and $|p=\frac{3}{2}\pi\rangle$ at each site. For $\lambda > -1$, the unperturbed ground state is

$$|G\rangle = \prod_j |p=0\rangle_j \ . \tag{4.4}$$

Note that the spin variable θ is disordered in this unperturbed ground state and we are in the high-temperature disordered phase. The potential U is a nearest-neighbor interaction. The effect of the operator θ_j on the eigenstates of p_j is

$$e^{im\theta_j}|p\rangle_j = |p + n\pi/2\rangle_j \ , \tag{4.5}$$

which is similar to Eq. (1.7). The ground-state energy per site is calculated in a series as

$$E(\lambda,\beta) = E^{(0)}(\lambda) + \beta E^{(1)}(\lambda) + \beta^2 E^{(2)}(\lambda) + \cdots \ . \tag{4.6}$$

The specific heat is obtained from the series (4.6) by differentiations

$$C(\lambda,\beta) = \frac{\partial^2}{\partial\beta^2} E(\lambda,\beta) \ . \tag{4.7}$$

2. Magnetizations and susceptibilities

Let us consider operators

$$O_m = \frac{1}{M}\sum_j D_m(j) \ , \tag{4.8}$$

where

$$D_m(j) = \prod_{k>j} e^{imp_k} \quad (m = \pm 1, 2) \ , \tag{4.9}$$

and M is the number of sites.

The operators $D_m(j)$ are dual to the operators $e^{im\theta_j}$ as seen from Eq. (2.11). They are called disorder operators and have nonzero expectation values in the high-temperature phase.[26] The disorder operators are convenient quantities to calculate in the high-temperature expansion. The expectation values of the operators $e^{im\theta_j}$ are zero in the high-temperature phase and the high-temperature expansion method cannot be applied to these quantities. For convenience sake we define

$$D_\pm = \prod_{k>j} \cos p_k \ . \tag{4.10}$$

To calculate series for magnetizations and susceptibilities of the operators $O_\pm = (1/M)\sum_j D_\pm(j)$ and $O_2 = (1/M)\sum_{ij} D_2(j)$, we add a magnetic field term to the Hamiltonian (4.1)

$$\mathcal{H} = T + hO_m + \beta U \ . \tag{4.11}$$

Although the new term hO_m is not diagonal, it can be formally included in the kinetic energy. The ground-state energy is calculated in a power series of β as before

$$E(\lambda,\beta;h) = E^{(0)}(\lambda;h) + E^{(1)}(\lambda;h)\beta + E^{(2)}(\lambda;h)\beta^2 + \cdots \ . \tag{4.12}$$

The terms up to second order in h are counted for $E^{(n)}(\lambda,h)$ because the physical quantities we are interested in are the magnetizations

$$\langle O_m \rangle = \left.\frac{\partial E(\lambda,\beta;h)}{\partial h}\right|_{h=0} \ , \tag{4.13}$$

and the susceptibilities

$$\langle O_m O_m \rangle = \left.\frac{\partial^2 E(\lambda,\beta;h)}{\partial h^2}\right|_{h=0} \ . \tag{4.14}$$

The series for the usual order operators are related to those for these disorder operators as, for example,

$$\frac{1}{M^2}\sum_j \langle e^{i2\theta_j}\rangle_\beta = \langle O_2 \rangle_{1/\beta} \ . \tag{4.15}$$

B. Results of series analysis

The 11th order perturbation calculations gave the following quantities: (1) free energy—12 terms (10 terms for the specific heat), (2) magnetization—12 terms, (3) susceptibility—10 terms. The series for susceptibilities are shorter because the 0th and 1st order perturbations for these quantities vanish.

The DLOG Padé method was applied to those series. Poles of Padé approximants give critical points and residues give critical indices. The estimates of critical points and critical indices were obtained by averaging four or five highest-order near diagonal elements $[n-1,n]$, $[n,n]$, and $[n+1,n]$ of Padé tables. The error bars are set to include those numbers. (The series and Padé table are not includ-

ed for reasons of space. They can be obtained on request from M.K.)

1. Critical lines

The best estimates for critical points are obtained from the series for the magnetization $\langle O_{\pm}\rangle$ and shown in Fig. 1. As λ becomes large the Padé tables become extremely stable and at $\lambda=4$ we estimate the critical value β_c as $\beta_c=0.490\,967\pm0.000\,009$. Also β_c approaches the Ising-type critical line $\beta=2/\lambda$ predicted in Sec. III. For $\lambda<1$, this analysis shows reasonably well-converged singularities around the self-dual line $\beta=1$. However, as λ approaches to $-\sqrt{2}/2$, where we predict the onset of the critical fan, the Padé tables become unstable. For $\lambda=-0.8$ and -0.9, where the Kosterlitz-Thouless type singularity is expected, we found poles as shown in Fig. 1.

An analysis for the other magnetization $\langle O_2\rangle$ gives almost the same quantitative results for $\lambda<1$. However for $\lambda>1$ the values of β_c from the $\langle O_2\rangle$ series are considerably larger than those from the $\langle O_{\pm}\rangle$ series. The differences are $0.1\sim0.15$ for $2\lesssim\lambda\lesssim4$. These poles, we think, do not represent singularities of $\langle O_2\rangle$ because the residues for these poles are unstable and small ($\approx10^{-3}$ at $x=4$) in the Padé tables for $\lambda\gtrsim3$. This result agrees with the phase diagram Fig. 1. Along the line 3, $e^{+i\theta_j}$ have singularities but $e^{i2\theta_j}$ has no singularity. Note that $\langle O_{\pm}\rangle$ and $\langle O_2\rangle$ are dual to those order variables and we expect no singularities for $\langle O_2\rangle$ along line 2 which is dual to line 3.

The estimates of critical points from the series for the susceptibilities $\langle O_{\pm}O_{\pm}\rangle$ and $\langle O_2O_2\rangle$ give qualitatively similar but slightly worse results. We think this is due to the shorter series for these quantities.

2. Critical indices

For $\lambda<1$, we know the exact critical point $\beta_c=1$. Instead of evaluating residues at poles, we can improve estimates of critical indices by evaluating Padé approximants of $(\beta-\beta_c)S^{-1}\partial S/\partial\beta$ at $\beta=\beta_c$. Here S is a series.

The extended scaling relations predict the critical indices α, β, and γ, with the help of the standard scaling relations for $-1<\lambda<1$. From Eqs. (3.9), (3.10), and (3.11) we have

$$x_T=\frac{\pi}{2}[\arccos(-\lambda)]^{-1}\ . \tag{4.16}$$

The standard scaling relations give

$$\alpha=2-\frac{2}{2-x_T}\ , \tag{4.17}$$

$$\beta_{\rm op}=\frac{x_{\rm op}}{2-x_T}\ , \tag{4.18}$$

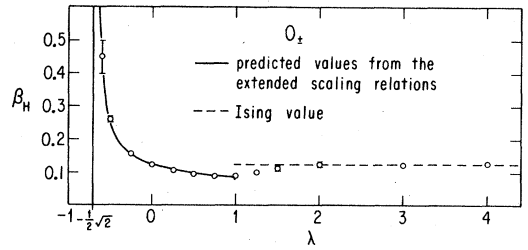

FIG. 3. Plots of series estimates of the critical index β for the operator $O_{\pm}$. At $\lambda=-\sqrt{2}/2$, β becomes infinity.

and

$$\gamma=\frac{2}{2-x_T}(1-x_{\rm op})\ , \tag{4.19}$$

where, $x_{\rm op}$ is given by Eqs. (3.12) and (3.13), namely,

$$x_{\rm op}=\begin{cases}\frac{1}{4}x_T, & \text{for } O_2\\ \frac{1}{8}, & \text{for } O_{\pm}\ .\end{cases} \tag{4.20}$$

The estimated critical indices are compared with those predictions.

In Figs. 3 and 4, β's for $O_{\pm}$ and O_2 are shown, respectively. They agree well with the extended scaling predictions. Also, the result from $\langle O_{\pm}\rangle$ series show a transition to the Ising value as λ becomes large.

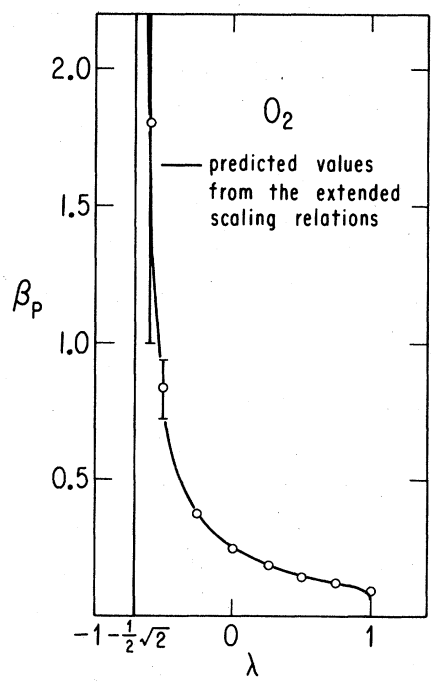

FIG. 4. Similar plots to Fig. 3 for the operator O_2.

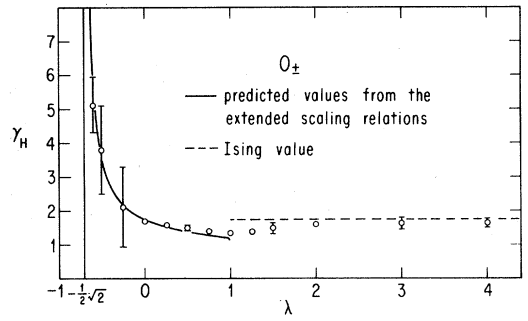

FIG. 5. Plots of series estimates of the critical index γ for the operator $O_{\pm}$. At $\lambda = 1\sqrt{2}/2$, γ becomes infinity.

The results for γ's are shown in Figs. 5 and 6. Finally the critical index α is shown in Fig. 7, which does not show a very good agreement with the extended scaling prediction. Also this does not show a well convergence to the Ising value $\alpha = 0$ as λ becomes large.

ACKNOWLEDGMENTS

We have had useful discussions with Steven Shenker, Robert Pearson, P. Rujan, and Bernhard Nienhuis. Pearson gave us Potts model data for checking our calculations. Rujan has obtained independently the results of the Appendix. We thank Michael Widom for assistance with the series analysis. One of us (M.K.) is grateful to T. Eguchi for useful discussions. Work supported by the University of Chicago Materials Research laboratory under Grant No. DMR 77-12637. One of us (M.d.N.) would like to acknowledge the support of the Netherlands Organization for the Advancement of Pure Research (ZWO).

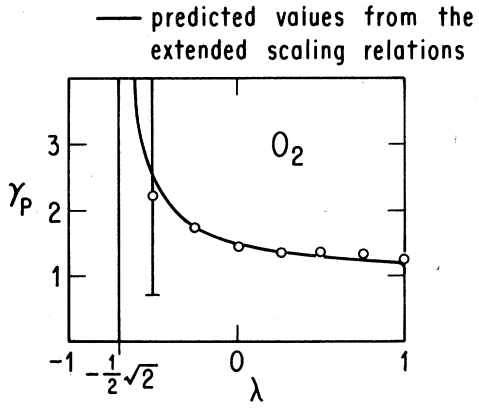

FIG. 6. Similar plots to Fig. 7 for the operator O_2.

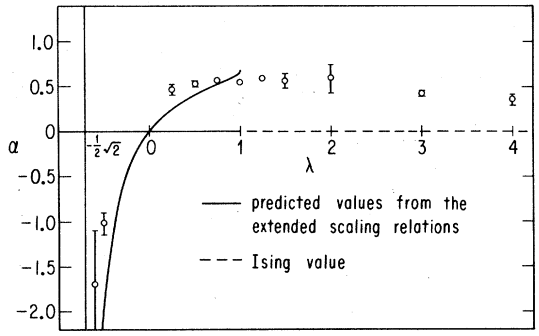

FIG. 7. Plots of series estimates of the critical index α. At $\lambda = -\sqrt{2}/2$, α becomes minus infinity.

APPENDIX

1. Mapping of the Ashkin-Teller model onto the six-vertex model

The six-vertex model[11] is a special case of the eight-vertex model,[14] which is defined by placing arrows on the bonds of a square lattice and allowing only those configurations with an even number of arrows pointing into each vertex. The Boltzmann weights of the eight possible vertex configurations are taken pairwise equal as shown in Fig. 8.

This model can also be represented as two Ising models coupled via a four-body interaction. The difference from the Ashkin-Teller model is that now the S and T spins are not located at the same lattice, but instead on each other dual lattice (see Fig. 9). One can translate the Ashkin-Teller model (with spins at the × sites in Fig. 9 into the eight-vertex model by a duality transformation on the T_i spins only.[13] The critical lines with continuously varying exponents of the two models are then found to map onto each other. However, changing the temperature

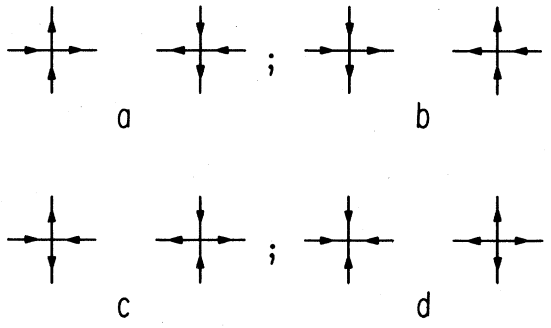

FIG. 8. Arrow configurations allowed at a vertex in the eight-vertex model.

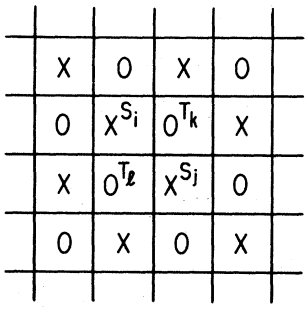

FIG. 9. Ising spin representation of the eight-vertex model. S spins are defined on sites × and T spins are defined on sites O.

is not the same in the two models. The energy operator of the eight-vetex model translates into the crossover operator, that makes the nearest-neighbor coupling K_2 for the S and T spins different. In the eight-vertex language on the other hand, the Ashkin-Teller energy operator leads to a staggering in the Boltzmann weights a and b.

For our purpose it is useful to combine this mapping with another one that maps the critical line of the eight-vertex model into the six-vertex model (where the Boltzmann weight $d=0$). In the language of this model one identifies moving along the critical line with changing the temperature. The eight-vertex temperature direction now corresponds to allowing d to become nonzero, while the Ashkin-Teller energy direction still leads to a staggering in a and b. For the isotropic square lattices all these relations are well known and, e.g., discussed in Ref. 6. They, however, also hold for the anisotropic cases.[10,27] The duality mappings can be carried out for any two-dimensional lattice type. The duality equations remain the same as for the isotropic case, one only has to add an index that denotes the specific vertex.[10]

The transformation of the anisotropic Ashkin-Teller model into the six-vertex model language is as follows. The Boltzmann weights for the two sublattices are

$$\begin{aligned} a_A &= e^{-2K_4^x}/\cosh 2K_2^x \ , \\ b_A &= \tanh 2K_2^x \ , \\ c_A &= 1 \ , \\ d_A &= 0 \ , \end{aligned} \tag{A1}$$

for sublattice A and

$$\begin{aligned} a_B &= \tanh 2K_2^\tau \ , \\ b_B &= e^{-2K_4^\tau}/\cosh 2K_2^\tau \ , \\ c_B &= 1 \ , \\ d_B &= 0 \ , \end{aligned} \tag{A2}$$

for sublattice B. The staggering vanishes when $a_A = a_B$ and $b_A = b_B$ which yields

$$\frac{e^{-2K_4^x}}{\cosh 2K_2^x} = \tanh 2K_2^\tau \ , \tag{A3}$$

$$\frac{e^{-2K_4^\tau}}{\cosh 2K_2^\tau} = \tanh 2K_2^x \ . \tag{A4}$$

These conditions are equivalent to

$$\beta = e^{2K_4^x + 2K_4^\tau} \sinh 2K_2^x \sinh 2K_2^\tau = 1 \tag{A5}$$

and

$$\Delta = -\frac{\sinh 2K_4^x}{\sinh 2K_2^x} = -\frac{\sinh 2K_4^\tau}{\sinh 2K_2^\tau} \ . \tag{A6}$$

In the six-vertex model the parameter Δ is defined as[11]

$$\Delta = \frac{a^2 + b^2 - c^2}{2ab} \ . \tag{A7}$$

The conditions (A5) and (A6) reduce to those of Eqs. (1.5) in the anisotropic limit $\tau \to 0$. The parameter λ in the Hamiltonian is identified to be the parameter $-\Delta$ in the vertex model. We conclude that the Hamiltonian (1.6) with $\beta = 1$ is equivalent to the six-vertex model.

2. Staggered *XXZ* model

There is another way of discussing the relationship with the six-vertex model. The six-vertex and eight-vertex model have a well-known quantum Hamiltonian of their own. We refer to the paper by Baxter[12] for the details of the derivation. In the anisotropy limit $b/a \to 0$ while keeping Δ fixed he finds for the six-vertex model the spin-$\frac{1}{2}$ Hamiltonian

$$H_{XXZ} = \sum_j [\, \sigma^x(j)\sigma^x(j+1) + \sigma^y(j)\sigma^y(j+1) + \Delta\sigma^z(j)\sigma^z(j+1)] \ . \tag{A8}$$

This is called the *XXZ* model. The parameter Δ is the same as the one defined in Eq. (A7). For the eight-vertex model ($d \neq 0$) the coefficients for the $\sigma^x(j)\sigma^x(j+1)$ and $\sigma^y(j)\sigma^y(j+1)$ terms are nonequal. This is the *xyz* model. Straightforward generalization of Baxter's method for the staggered six-vertex model of Eqs. (A1) and (A2) leads to the

staggered XXZ model[21]

$$H_{XXZ}=\sum_j[1+(-1)^j t]\times[\sigma^x(j)\sigma^x(j+1)+\sigma^y(j)\sigma^y(j+1)+\Delta\sigma^z(j)\sigma^z(j+1)] \quad . \tag{A9}$$

From the discussion in the Appendix Sec. 1 we know that this must be equivalent to our Ashkin-Teller Hamiltonian. Indeed we can rewrite $\mathcal{H}_{AT}$ into this form. Start by rewriting the Ashkin-Teller Hamiltonian (1.6) in terms of the Pauli spin matrices $\sigma_S^{x,z}$ and $\sigma_T^{x,z}$ (see Table II).

TABLE II. Eigenvalues of the Pauli spin operators

θ	σ_S^z	σ_T^z	$\sigma_S^z\sigma_T^z$
0	1	1	1
$\pi/2$	1	−1	−1
π	−1	−1	1
$3\pi/2$	−1	1	−1

$$\mathcal{H}_{AT}=\sum_j\{[1-\sigma_S^x(j)]+[1-\sigma_T^x(j)]+\lambda[1-\sigma_S^x(j)\sigma_T^x(j)]\}$$
$$-\beta\sum_j[\sigma_S^z(j)\sigma_S^z(j+1)+\sigma_T^z(j)\sigma_T^z(j+1)+\lambda\sigma_S^z(j)\sigma_S^z(j+1)\sigma_T^z(j)\sigma_T^z(j+1)] \quad . \tag{A10}$$

First remember that the Ashkin-Teller model is mapped into the eight-vertex model by a duality transformation on the T spins only. In the quantum case this is obtained by the duality transformation

$$\sigma_T^z(j+\tfrac{1}{2})=\prod_{k=1}^{j}\sigma_T^x(k) \quad , \qquad \sigma_T^x(j+\tfrac{1}{2})=\sigma_T^z(j+1)\sigma_T^z(j) \quad . \tag{A11}$$

The result is

$$\mathcal{H}_{AT}=-\sum_j\{\sigma_T^z(j+\tfrac{1}{2})\sigma_T^z(j-\tfrac{1}{2})+\sigma_S^x(j)+\beta[\sigma_T^x(j+\tfrac{1}{2})+\sigma_S^z(j)\sigma_S^z(j+1)]$$
$$+\lambda[\sigma_T^z(j-\tfrac{1}{2})\sigma_S^x(j)\sigma_T^z(j+\tfrac{1}{2})+\beta\sigma_S^z(j)\sigma_T^x(j+\tfrac{1}{2})\sigma_S^z(j+1)]\} \quad . \tag{A12}$$

We can drop the S and T indices because we have a string of spins, separated by half the original lattice constant. Now once again apply the dual transformation of the type (A11) to all spins. This gives

$$\mathcal{H}_{AT}=-\sum_j\{\sigma^x(j+\tfrac{1}{4})\sigma^x(j-\tfrac{1}{4})+\sigma^z(j+\tfrac{1}{4})\sigma^z(j-\tfrac{1}{4})-\lambda\sigma^y(j+\tfrac{1}{4})\sigma^y(j-\tfrac{1}{4})$$
$$+\beta[\sigma^x(j+\tfrac{1}{4})\sigma^x(j+\tfrac{3}{4})+\sigma^z(j+\tfrac{1}{4})\sigma^z(j+\tfrac{3}{4})-\lambda\sigma^y(j+\tfrac{1}{4})\sigma^y(j+\tfrac{3}{4})]\} \quad . \tag{A13}$$

Here we used $i\sigma^y=\sigma^z\sigma^x$. This is the staggered XXZ model that we were looking for. To obtain Eq. (A9) we only need to apply the rotation: $\sigma^z\to\sigma^y$ and $\sigma^y\to-\sigma^z$. As before we find that the parameter Δ of the six-vertex model is equal to $-\lambda$.

---

*Presented as a thesis to the Department of Physics, The University of Chicago, in partial fulfillment of the requirement for the Ph.D. degree. Present address: Department of Physics, FM15, University of Washington, Seattle, Wash. 98195.

[1]J. Ashkin and E. Teller, Phys. Rev. 64, 178 (1943).
[2]For a review, see J. Kogut, Rev. Mod. Phys. 51, 659 (1979).
[3]L. Onsager, Phys. Rev. 65, 117 (1944).
[4]R. J. Baxter, J. Phys. C 6, L445 (1973).
[5]I. G. Enting, J. Phys. A 8, 1681 (1975).
[6]M. den Nijs, J. Phys. A 12, 1957 (1979).
[7]B. Nienhuis, E. K. Riedel, and M. Schick, J. Phys. A 13, L189 (1980); R. B. Pearson (unpublished).
[8]H. J. F. Knops, J. Phys. A 8, 1508 (1975).
[9]F. Y. Wu and K. Y. Lin, J. Phys. C 7, L181 (1974).
[10]M. den Nijs, thesis (1979) (unpublished).
[11]E. H. Lieb, Phys. Rev. Lett. 18, 692, 1046 (1967); Phys. Rev. Lett. 19, 108 (1967). For a review see, E. H. Lieb and F. Y. Wu, in *Phase Transitions and Critical Phenomena*, edited by C. Domb and M. S. Green (Academic, London, 1972), Vol. 1.
[12]R. J. Baxter, Ann. Phys. (N.Y.) 70, 323 (1972).
[13]F. J. Wegner, J. Phys. C 5, L131 (1972).
[14]R. J. Baxter, Phys. Rev. Lett. 26, 832 (1971).
[15]M. Barber and R. Baxter, J. Phys. C 6, 2913 (1973).
[16]L. P. Kadanoff, Phys. Rev. Lett. 39, 903 (1977).
[17]L. P. Kadanoff, Ann. Phys. (N.Y.) 120, 39 (1979).

[18]L. P. Kadanoff and A. Brown, Ann. Phys. (N.Y.) 121, 318 (1979).
[19]H. J. F. Knops, Ann. Phys. (N.Y.) 128, 448 (1981).
[20]A. Luther and I. Peschel, Phys. Rev. B 12, 3908 (1975).
[21]M. den Nijs, Phys. Rev. B (in press).
[22]J. L. Black and V. J. Emery, Phys. Rev. B 23, 429 (1981).
[23]J. M. Kosterlitz, J. Phys. C 7, 1046 (1974).
[24]J. V. José, L. P. Kadanoff, S. Kirkpatrick, and D. Nelson, Phys. Rev. B 16, 127 (1977).
[25]L. P. Kadanoff and M. Kohmoto, J. Phys. A 14, 1291 (1981).
[26]L. P. Kadanoff and H. Ceva, Phys. Rev. B 3, 3918 (1971); L. P. Kadanoff and M. Kohmoto, Nucl. Phys. B (in press).
[27]F. J. Wegner, Physica (Utrecht) 68, 570 (1973).